Development of a Shock Loading Simulation Facility

K.D. Gardner, A.G. John, and F.K. Lu

Aerodynamics Research Center, Mechanical and Aerospace Engineering Department, Box 19018, University of Texas at Arlington, Arlington, TX 76019, USA

Abstract. A shock loading facility for simulating blast effects on construction materials has been developed. This facility was modified from an existing, conventional shock tunnel. It comprises of a driver section (3 m long, 0.15 m bore), a double diaphragm section and a driven section (8.23 m long, 0.15 m bore). A concrete specimen holder is placed in the test section. Downstream of the test section is a diffuser pipe followed by a vacuum tank. Concrete specimens of 305 mm length and 152 mm diameter can be tested. Test pressures ranged from 550–1600 kPa. Two transducers were mounted in the driven section to obtain time-of-flight measurements of the propagating shock wave. The test section houses a single concrete cylinder with embedded strain gauges. The concrete specimens were instrumented with four strain gauges to provide a qualitative indication of shock strength attenuation. The facility is capable of producing a blast wave equivalent to a TNT explosion of various mass and distance; for instance, 2 kg TNT at a range of 5 m or 214 kg TNT at 20 m.

1 Introduction

The past decade has brought an increased level of terrorist attacks throughout the world. A common form of attack is an improvised explosive device employed against a civilian structure. Blast waves resulting from the explosive burst in air causes severe structural damage to buildings that often collapse before evacuation is possible. Primary damage results from blast wave reflection when pressure is amplified through multiple reflections in multiphase media or in confined geometries. There are certain unique features of terrorist bombs, ranging in size, quality, sophistication and effectiveness. Thus, the basic principles of shock dynamics can be applied specifically to understand the effects of terrorist-type bombs on common building materials. Ultimately, it is necessary to design civilian structures to mitigate the effects of such weapons.

A blast wave simulator provides a safe environment to gain insight into blast effects and test numerical simulations. Such a simulator allows the specimen to be tested under low loadings prior to further testing with high explosives. This approach reduces the need for expensive full-scale or field testing while, at the same time, allows meaningful data to be gathered. Such a facility has been developed to study the effect of shock waves on concrete by modifying a hypersonic shock tunnel. Detonation of high explosive materials in free air creates a blast wave whose overpressure can be simulated by a shock wave. The primary difference is that the blast profile is one of a pressure spike followed by a steady decay, whereas that of a shock wave is a sustained pressure loading of short duration. However, to obtain a qualitative understanding of blast effects on materials, this difference may not be too significant.

Two avenues of investigation are currently being pursued with the facility. One involves using a weak sand–cement mixture as a protective damping material. Protection of existing structures could be provided by constructing a secondary outer wall composed of such a material. The secondary wall provides a sacrificial barrier to absorb

blast wave energy. A second investigation involves development and implementation of concrete embedded sensors. The embedded sensors provide data regarding attenuation coefficients for specific materials. The attenuation coefficients are needed for accurate numerical simulations of blast wave interaction.

2 Theory of Simulator Operation

The basic shock tube has been exploited as a practical research tool for over a century. The mechanics are well understood and explained in many gasdynamics texts [1]. The shock tube basically consists of two main sections, the driver and driven sections. A large pressure difference initially exists between the two sections. High pressure in the driver section and low pressure in the driven section are separated by a diaphragm. The diaphragm is ruptured, creating a contact surface between high pressure and low pressure. A normal one-dimensional shock wave arises from the pressure discontinuity and propagates into the driven section at Mach number M_s.

One-dimensional wave theory is used to obtain the resulting shock wave properties and flow conditions. The primary parameter concerning shock wave properties is the initial driver-to-driven pressure ratio P_4/P_1. The pressure ratio across the shock wave P_2/P_1 is determined from the basic shock tube equation

$$\frac{P_4}{P_1} = \frac{P_2}{P_1}\left[1 - \frac{(\gamma_4 - 1)(a_1/a_4)(P_2/P_1 - 1)}{\sqrt{2\gamma_1}\sqrt{2\gamma_1 + (\gamma_1 + 1)(P_2/P_1 - 1)}}\right]^{-2\gamma_4/(\gamma_4 - 1)} \tag{1}$$

and the Mach number M_s of the incident shock is given by

$$M_s = \sqrt{\frac{\gamma_1 + 1}{2\gamma_1}\left(\frac{P_2}{P_1} - 1\right) + 1} \tag{2}$$

The total pressure P_0 of flow behind the shock wave is given by

$$P_0 = P_2\left(1 + \frac{\gamma_1 - 1}{2}M_s^2\right)^{\gamma_1/(\gamma_1 - 1)} \tag{3}$$

The shock wave propagates through the driven tube at M_s until it encounters a nozzle through which the cross-sectional diameter increases. The flow is isentropically expanded through the nozzle, causing the Mach number to increases while total pressure is conserved. Therefore, shock wave total pressure in the test section is the same as the total pressure in the driven tube.

Two pressure transducers placed 344.6 and 481.8 cm from secondary diaphragm, located toward at the downstream end of the driven tube provide shock wave static pressures and arrival times. From the arrival time at two locations and the distance between them, the Mach number of the shock wave can be calculated from

$$M_s = \frac{d}{t_{PT2} - t_{PT1}}(\gamma_1 R_1 T_1)^{-1/2} \tag{4}$$

where t_{PT2} and t_{PT1} are arrival times at the two transducers, d is the distance between them, γ_1 is the ratio of specific heats for air, R_1 is the gas constant for air, and T_1 is the temperature of air in the driven tube. The uncertainty for this measurement is given by

$$\left(\frac{\Delta M_s}{M_s}\right) = \left(\frac{\Delta d}{d}\right)^2 + \left(\frac{\Delta t}{t_{PT2} - t_{PT1}}\right) + \frac{1}{4}\left(\frac{\Delta T_1}{T_1}\right) \tag{5}$$

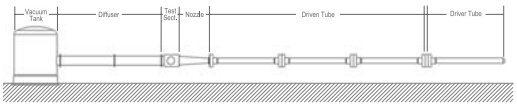

Fig. 1. Components of the blast wave simulator facility (flow from right to left).

where the Mach number uncertainty ΔM_s is a function of distance uncertainty Δd, time uncertainty Δt, and temperature uncertainty ΔT. The uncertainty of P_0 is given by

$$\left(\frac{\Delta P_0}{P_0}\right) = \left(\frac{\Delta P_2}{P_2}\right)^2 + \left(\frac{2\gamma_1}{\gamma_1 - 1}\right)\left(\frac{\Delta M_s}{M_s}\right)^2 \tag{6}$$

where ΔP_2 is uncertainty in P_2.

When high explosive materials are detonated, very high local pressures are created. The sudden pressure disturbance develops into a spherical shock wave. The blast wavefront possesses a peak pressure followed by a decay, while the shock wave created by a shock tunnel is a pressure step of some duration. Although there is a difference in the two pressure profiles, the peak pressure of the shock tunnel can be used to simulate that of the blast wave provided that the duration is not too long. This short pulse duration is typically encountered in nonreflected shock tunnels with a few milliseconds of run time. Smith and Hetherington [2] discuss wavefront parameters and scaling laws. They listed correlations where the pressure is equivalent to a certain TNT charge at a distance. Thus, the wavefront static pressure P_2 in kPa is given by

$$P_2 = 101.325 + \frac{1407.2}{Z} + \frac{554}{Z^2} - \frac{35.7}{Z^3} + \frac{0.625}{Z^4} \qquad (0.05 \le Z \le 0.3) \tag{7}$$

$$= 101.325 + \frac{619.4}{Z} - \frac{32.6}{Z^2} + \frac{213.2}{Z^3} \qquad (0.3 \le Z \le 1) \tag{8}$$

$$= 101.325 + \frac{66.2}{Z} + \frac{405}{Z^2} + \frac{328.8}{Z^3} \qquad (1 \le Z \le 10) \tag{9}$$

The scaled distance parameter Z is given by

$$Z = R/W^{1/3} \tag{10}$$

where R is the distance from the charge center in meters and W is the charge mass in kilograms of TNT. With the Z parameter, an equivalent blast strength and range is determined for each simulation.

3 Facility Description

The blast wave simulator is basically a non-reflected shock tunnel in which a concrete test specimen is directly exposed to a shock wave. The main components include a driver tube, driven tube, expansion nozzle, test section, diffuser, and vacuum tank, shown schematically in Fig. 1.

The driver tube is 3 m in length and it has an internal diameter of 15.2 cm. This tube may be pressurized to 41.3 MPa. The driven tube section consists of three segments with a total length of 8.23 m. The driven tube also has an internal diameter of 15.2 cm. It may be vacuumed to an absolute pressure of as low as 3.4 kPa. Between the driver and driven

tubes lies an intermediate tube section 11.4 cm long. The intermediate section pressure is initially held at half the driver section pressure. Thin metal diaphragms separate the three sections, as shown schematically in Fig. 2.

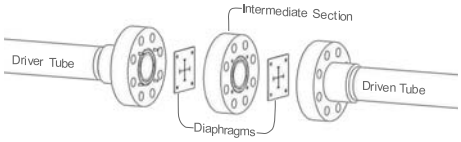

Fig. 2. Exploded view of diaphragm section shows the driver section diaphragm (left) and intermediate section diaphragm (right). Upon diaphragm rupture, air flows from the high pressure section (left) to the low pressure section (right).

Decreasing the intermediate section pressure causes the driver section diaphragm to rupture, which is immediately followed by the rupture of the intermediate section diaphragm. A strong shock wave is generated by the sudden large pressure difference. The shock wave propagates into the low pressure (driven) section at supersonic velocity. This process is shown in Fig. 3.

The end of the driven tube connects to an expansion nozzle, increasing the cross-sectional diameter from 15.2 cm to 30.5 cm through an axial distance of 117 cm. The test section is 55.9 cm long and it possesses 23 cm diameter circular access ports on either side. The test section houses a conical converging section which leads into the diffuser. Flow exiting the diffuser continues into a vacuum tank. The vacuum tank has volume of 4.25 m^3 and it has a high flow-rate check valve for automatic pressure relief.

The test section accommodates a 30.5 cm long by 15.2 cm diameter concrete cylinder. The cylinder is mounted facing normal to an incoming shock wave. The cylinder is mounted in a steel shell that has a length of 30.5 cm and an internal diameter of 17.8 cm. A ring on the distal end of the tube provides support against axial movement. Contact between the cylinder and ring surfaces is damped by a 1.3 cm thick neoprene pad. The gap around the cylinder circumference is filled with an expanding polyurethane foam. The neoprene and polyurethane materials hold the specimen securely while damping both stress wave concentration and interaction with boundaries. Only the front (circular) surface of the cylinder is exposed perpendicularly to the incident shock. Most of the rear cylinder surface is also unbounded in order to lessen stress wave transmission through the rear boundary and to allow scabbing of the specimen.

3.1 Diaphragm Development

The diaphragm bursting pressure directly influences the total pressure and thus the load delivered to a concrete specimen. On the other hand, shock wave strength is directly related to the initial pressure ratio across the diaphragms P_4/P_1. Non-destructive testing capability is an important objective in the development of the blast loading facility. High loads may cause the formation of fractures in the specimens which may interfere with internal stress waves. Such fractures are difficult to detect without extensive additional inspection following each simulation. High loads may also cause structural deformation of the test section which is not designed for high loads. Therefore, high bursting pressure is unnecessary and undesirable.

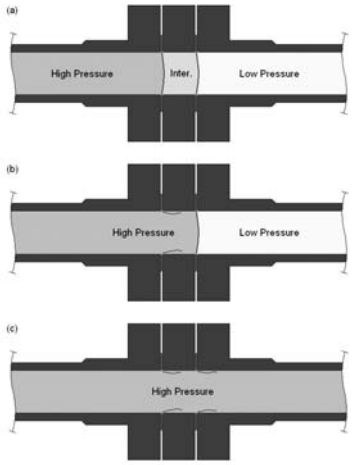

Fig. 3. The diaphragm rupture process. It begins with three initially separate regions (a). Pressure in the intermediate section is decreased to increase the pressure difference across the driver diaphragm (b). The ensuing rupture causes an equal pressure difference across the intermediate diaphragm (c).

Diaphragms previously developed for the shock tunnel possessed bursting pressures as low as 2.07 MPa, which is too high for the present application. A series of tests was performed to determine the usability and rupture pressures of different diaphragm materials. It was found that 0.41 mm aluminum shim stock exhibited bursting pressures that are both consistent and desirable, ranging from 1.00–1.09 MPa with a 1.04 MPa mean.

These diaphragms were easy to fabricate compared to the steel diaphragms. A paper cutter or tin snips may be used to cut the shim stock into 15.24 cm squares. A punch tool was fabricated and used to punch 12.7 mm dowel holes for alignment.

3.2 Data Acquisition

Data is acquired with a 12-bit, 48 channel, simultaneous sample-and-hold system operating at 100 kHz each, supplemented by eight channels at 1 MHz each. An external trigger signal is supplied by a piezoelectric pressure transducer mounted in the driven tube. Data is transferred to a host computer for reduction and analysis via a bus extender.

The facility is currently instrumented with several types of pressure transducers. Three PCB piezoelectric pressure transducers are flush mounted in the driven tube. Two provide shock wave static pressure and time of arrival. The third serves as the external trigger signal to the data acquisition system. These PCB model 111A24 transducers have 0.14 kPa resolution and 2 μs rise time.

4 Results and Conclusions

Figure 4 shows readings from two pressure transducers along the driven tube. The first transducer reading shows a relatively slow rise in pressure upon wave front arrival. How-

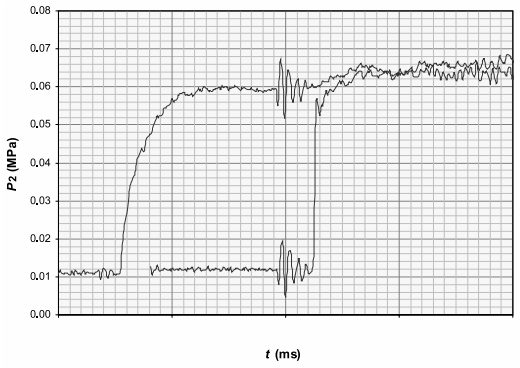

Fig. 4. Pressure profile from pressure transducers along the driven tube.

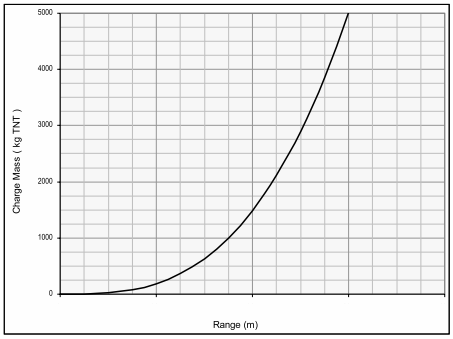

Fig. 5. Blast waves equivalent to the pressure data of Fig. 4.

ever, by the time the wave front reaches the second transducer downstream, it has developed a much sharper pressure increase. The initial driver pressure was 1.41 ± 0.056 MPa and the initial driven pressure was 0.01 ± 0.0004 MPa. The distance between the pressure transducers is 1.37 ± 0.001 m. The shock Mach number was calculated from Eqns. (4) and (5) to be 2.36 ± 0.026. From the experimental data in Fig. 4, a P_2 value of approximately 0.06 MPa is obtained. Using this value and Eqns. (7)–(9), equivalent blast waves are shown in Fig. 5.

Acknowledgements

The support of the U.S. Civilian Research and Development Foundation through Grant No. Grant No. RE2-2381-MO-02 is gratefully acknowledged.

References

1. H.W. Liepmann and A. Roshko: *Elements of Gasdynamics*, Wiley, New York (1957)
2. P.D. Smith and J.G. Hetherington: *Blast and Ballistic Loading of Structures*, Butterworth-Heinemann, Oxford (1994)